MNRAS **485,** L136–L140 (2019)
Advance Access publication 2019 March 19
doi:10.1093/mnrasl/slz039

Detection of a giant white-light flare on an L2.5 dwarf with the Next Generation Transit Survey

James A. G. Jackman [1,2]★ Peter J. Wheatley [1,2] Daniel Bayliss [1,2] Matthew R. Burleigh,[3] Sarah L. Casewell,[3] Philipp Eigmüller,[4,5] Mike R. Goad,[3] Don Pollacco,[1,2] Liam Raynard [3] Christopher A. Watson[6] and Richard G. West [1,2]

[1]*Department of Physics, University of Warwick, Gibbet Hill Road, Coventry CV4 7AL, UK*
[2]*Centre for Exoplanets and Habitability, University of Warwick, Gibbet Hill Road, Coventry CV4 7AL, UK*
[3]*Department of Physics and Astronomy, University of Leicester, University Road, Leicester LE1 7RH, UK*
[4]*Institute of Planetary Research, German Aerospace Center, Rutherfordstrasse 2, D-12489 Berlin, Germany*
[5]*Center for Astronomy and Astrophysics, TU Berlin, Hardenbergstr. 36, D-10623 Berlin, Germany*
[6]*Astrophysics Research Centre, School of Mathematics and Physics, Queen's University Belfast, Belfast BT7 1NN, UK*

Accepted 2019 March 14. Received 2019 March 13; in original form 2019 February 4

ABSTRACT

We present the detection of a $\Delta V \sim -10$ flare from the ultracool L2.5 dwarf ULAS J224940.13−011236.9 with the Next Generation Transit Survey (NGTS). The flare was detected in a targeted search of late-type stars in NGTS full-frame images and represents one of the largest flares ever observed from an ultracool dwarf. This flare also extends the detection of white-light flares to stars with temperatures below 2000 K. We calculate the energy of the flare to be $3.4^{+0.9}_{-0.7} \times 10^{33}$ erg, making it an order of magnitude more energetic than the Carrington event on the Sun. Our data show how the high-cadence NGTS full-frame images can be used to probe white-light flaring behaviour in the latest spectral types.

Key words: stars: flare – stars: individual: ULAS J224940.13−011236.9 – stars: low-mass.

1 INTRODUCTION

Previous studies of L dwarfs ($T_{\rm eff}$ = 1300–2300 K; Stephens et al. 2009) have shown them to be variable in a number of ways. Examples of this include periodic modulation due to clouds (e.g. Gizis et al. 2015), radio emission due to aurora in late L dwarfs (e.g. Kao et al. 2018), and the presence of white-light flares (e.g. Gizis et al. 2013). White-light flares occur through reconnection events in the stellar magnetic field, which result in heating of the lower chromosphere/upper photosphere (e.g. Benz & Güdel 2010), resulting in white-light emission. While seen regularly on GKM stars, observations of white-light flares on L dwarfs remain rare, with only a handful of stars showing them to date (e.g. Paudel et al. 2018). However, those observed have included some of the largest amplitude flares ever recorded, reaching up to $\Delta V \approx -11$ (Schmidt et al. 2016). This shows that white-light flaring activity persists into the L spectral type, despite previous studies of L dwarfs showing their chromospheres and magnetic activity to be diminished compared to those of late M dwarfs (e.g. Schmidt et al. 2015).

Because of the rarity of these large amplitude flares, long duration observations are required when targeting L dwarfs specifically. This became possible with the *Kepler* (Borucki et al. 2010) and *K2* (Howell et al. 2014) missions, which allowed continuous high precision monitoring of chosen objects (Gizis et al. 2013, 2017a; Paudel et al. 2018). Through this, large amplitude flares ($\Delta V \approx -8$, $\Delta K_{\rm p} = -5.4$) were detected on an L0 and L1 dwarf (Gizis et al. 2017a; Paudel et al. 2018), along with smaller flares on two early L dwarfs (Gizis et al. 2013; Paudel et al. 2018). Spectroscopy of an L5 dwarf by Liebert et al. (2003) showed an Hα flare, although this event lacked the continuum enhancement associated with white-light flares. Observations of an L5 dwarf (Gizis et al. 2017b) with *K2* showed no detectable white-light flares, suggesting such events are suppressed at late spectral types. For targeted observations it is typically required that the star be visible in quiescence. For optical surveys that are not sensitive to late spectral types, this requirement limits observations to a small number of nearby early L dwarfs.

Wide-field surveys (e.g. All-Sky Automated Survey for Supernovae, ASAS-SN) that obtain full-frame images of large areas of sky per night allow studies to push to fainter stars. In these surveys, full-frame images can be used to search for very faint stars that only become detectable when flaring. This led to the detection of a $\Delta V \approx -11$ flare from the L0 dwarf ASASSN-16ae (Schmidt et al. 2016), previously the only L dwarf flare detected from the ground with optical photometry. While these surveys can detect large flares, the low-cadence light curves limit the study of shape and substructure, and hence also the accuracy of flare energy

★ E-mail: J.Jackman@warwick.ac.uk

calculations (e.g. Schmidt et al. 2018). Consequently, in order to detect and characterise the largest flare events on the latest spectral types, high-cadence wide-field observations with full-frame images are required.

In this Letter, we present the detection of a white-light superflare from the L2.5 dwarf ULAS J224940.13−011236.9, which was observed at high cadence with the Next Generation Transit Survey (NGTS). This source has also previously been identified as 2MASS J22494010−0112372. We describe the detection of the flare and how we derived the properties of the flare and the host star.

2 OBSERVATIONS

NGTS is a ground-based wide-field exoplanet survey, which obtains full-frame images from 12 independent telescopes at 12 s cadence (Wheatley et al. 2018). The telescopes have apertures of 20 cm and operate with a bandpass of 520–890 nm. They have a total instantaneous field of view of 96 deg^2.

The data presented in this Letter were collected with NGTS between 2017 May 7 and 2017 December 14, comprising 146 nights of data. The detected flare occurred on the night of 2017 August 13.

2.1 Input catalogue and flare detection

In the normal mode of operations NGTS obtains light curves for all stars brighter than $I = 16$ (Wheatley et al. 2018). However, in each NGTS field there exist on average 2500 red stars fainter than this limit that can be identified using Two Micron All Sky Survey (2MASS; Skrutskie et al. 2006) and *Gaia* (Gaia Collaboration et al. 2018). While too faint to observe as primary targets, by placing photometric apertures on their positions we can capture any variability, such as flares, that may result in them becoming bright enough to detect. To this end, for each NGTS field we compiled input catalogues of known red stars using positions from 2MASS and the colour cuts for ultracool dwarfs specified by Muirhead et al. (2018). The normal NGTS pipeline (Wheatley et al. 2018) was then run on these positions. To search for flares we follow the procedure of Jackman et al. (2018) and look for consecutive outliers 6 median absolute deviations (MAD) above the median of a single night.

Using this method we detected a flare from the star ULAS J224940.13−011236.9 (Skrzypek, Warren & Faherty 2016, hereafter ULAS J2249−0112), shown in Fig. 1. To confirm this star is the source of the flare, we checked the centroiding of this source, along with the NGTS images before, during and after the flare. We can see no measurable centroid shift during the flare and do not identify any brightening from a nearby source or from a satellite passing through our aperture. Consequently, we are confident the detected flare comes from ULAS J2249−0112.

2.2 Stellar properties

ULAS J2249−0112 has previously been identified as an L2.5(±1) dwarf by Skrzypek et al. (2016), as part of a sample of photometrically classified L and T dwarfs from Sloan Digital Sky Survey (SDSS; York et al. 2000), UKIRT Infrared Deep Sky Survey (UKIDSS; Lawrence et al. 2007), and *Wide-field Infrared Survey Explorer* (*WISE*; Wright et al. 2010). To confirm this and measure the effective temperature of ULAS J2249−0112, we fit the spectral energy distribution (SED) using the BT-Settl models (Allard, Homeier & Freytag 2012). We fit to the catalogue photometry in Table 1, following a similar method to Gillen et al. (2017). We note here that this source is too faint to be detected by *Gaia*. From our fitting we measure an effective temperature of $T_{\rm eff} = 1930 \pm 100$ K, consistent with that expected for the L2.5 spectral type (Stephens et al. 2009).

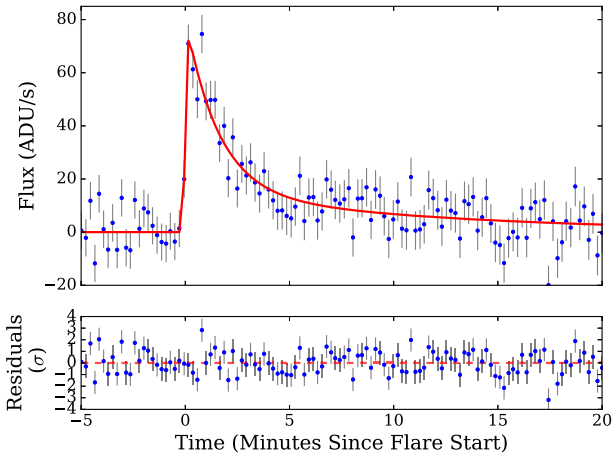

Figure 1. Top: NGTS light curve of the flare from ULAS J2249−0112. Blue points are NGTS photometry, and the best-fitting model is overlaid in red. Note the outlier near the flare peak, something we discuss further in Section 4.2. Bottom: residuals from the model fit.

Table 1. Properties of ULAS J224940.13−011236.9. References: 1 – Skrutskie et al. (2006); 2 – Bramich et al. (2008); 3 – Cutri & et al. (2014).

Property	Value	Reference
RA (J2000, °)	342.417115	1
Dec. (J2000, °)	−1.210352	1
i'	21.461 ± 0.101	2
z'	19.627 ± 0.102	2
J	16.832 ± 0.138	1
H	16.065 ± 0.177	1
K_s	15.610 ± 0.215	1
$W1$	15.091 ± 0.037	3
$W2$	14.775 ± 0.082	3
$\mu_{\rm RA}$ (mas yr^{-1})	87.4 ± 4.2	2
$\mu_{\rm Dec.}$ (mas yr^{-1})	22.6 ± 4.2	2
$T_{\rm eff}$ (K)	1930 ± 100	This work
Distance (pc)	76^{+8}_{-7}	This work
Radius ($R_\odot$)	0.10 ± 0.02	This work

ULAS J2249−0112 was also observed by the Baryon Oscillation Spectroscopic Survey (BOSS; Dawson et al. 2013). BOSS obtains optical spectra with a resolution of $R \approx 2000$ over a wavelength range 3600–10 000 Å. ULAS J2249−0112 also sits in SDSS stripe 82; however, due to its faint i magnitude was not included in the analysis of BOSS ultracool dwarfs by Schmidt et al. (2015). We excluded wavelengths below 5400 Å in our analysis due to the lack of emission in the blue from ULAS J2249−0112.

Fitting this spectrum using the empirical L dwarf templates of Schmidt et al. (2015) gives a best-fitting spectral type of L2.6 ± 0.1, again confirming our spectral type determination and the low temperature. The BOSS spectrum with the best-fitting template is shown in Fig. 2. Because of the low signal-to-noise (S/N) ratio (1.2 around Hα) of the spectrum we are not able to clearly identify the presence of Hα emission in quiescence.

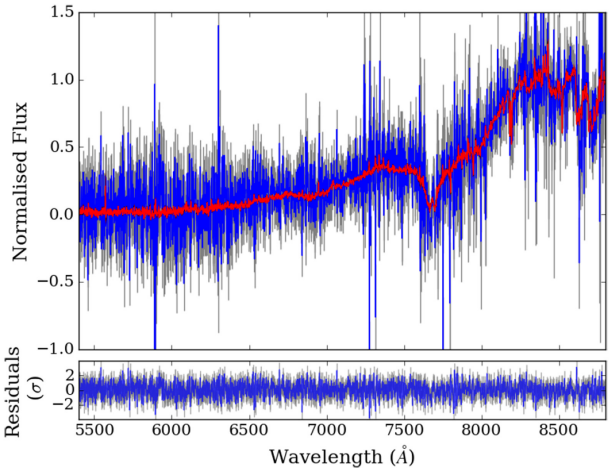

Figure 2. Top: BOSS spectrum of ULAS J2249−0112 in blue, with errors in grey. The spectrum has been normalised at 8350–8450 Å with the best-fitting L-dwarf template overlaid in red. Bottom: residuals from the fit.

2.2.1 *Kinematics*

In order to estimate the distance to ULAS J2249−0112 we initially calculate the absolute 2MASS and *WISE* magnitudes using the relations of Dupuy & Liu (2012), derived from ground-based infrared astrometry, using the L2.5 spectral type. When calculating the distances using these individual absolute magnitudes, we found all calculated distances to be consistent. We thus took a weighted mean of the individual photometric distances, which we calculate as 76^{+8}_{-7} pc. For the proper motion we have used the measurements of Bramich et al. (2008), which are given in Table 1. These values were obtained using the repeat measurements of ULAS J2249−0112 as part of SDSS stripe 82. For the radial velocity we have used the value provided with the BOSS spectrum, $v_{\rm rad} = -14 \pm 10$ km s^{-1}. By combining these values together we calculate the three-dimensional velocities $(U, V, W) = (-33.5 \pm 4.2, -10.3 \pm 6.1, 0.5 \pm 7.9)$ km s^{-1}. These values appear to place ULAS J2249−0112 within the thin disc (Schmidt et al. 2010; Burgasser et al. 2015).

3 RESULTS

3.1 Amplitude and duration

To determine the amplitude and duration of the flare, and to search for signs of substructure, we fit the NGTS data with the solar-flare inspired model from Jackman et al. (2018). This model incorporates both a Gaussian heating term and a double exponential for the flare cooling. We fit the model using a Markov chain Monte Carlo (MCMC) process with 100 walkers for 20 000 steps. We disregard the first 1000 steps as a burn-in. The result of this fit is shown in Fig. 1. From looking at the residuals to the fit we can identify a single outlier around the flare peak that may be signs of partially resolved flare substructure, something we discuss further in Section 4.2. We use the best-fitting model to measure the duration for which the flare is at least 1σ above the background, where σ is the standard deviation of the light curve when the star is in quiescence. We measure the visible duration as 9.5 min. We can use also use our fit to measure the e-folding time-scale and the $t_{1/2}$ duration of the flare. These parameters are often used in flare analysis (e.g. Shibayama et al. 2013; Davenport et al. 2014) and provide separate measures of the duration. We measure these as 2.1 and 1.5 min, respectively. The full width at half-maximum (FWHM) of the Gaussian heating term also gives a measure of the flare rise time, something not typically measured in other surveys due to its short duration. We find this to be 12 s, indicating rapid heating.

We can also use our fitted model to measure the amplitude of the flare, using the peak count rate. In order to determine what magnitude this corresponds to (in order to calculate the fractional amplitude of the flare) we have cross-matched all NGTS sources in this field with SDSS to obtain a linear relation between the NGTS instrumental magnitude and SDSS i' band. Using this relation we convert the NGTS instrumental flux to a proxy i' band magnitude of 15.3, resulting in $\Delta i' \simeq -6$. For comparison with previous works on large L dwarf flares, we also estimate the magnitude in the V band. To do this we use the best-fitting BT-Settl model and assume the flare is given by a 9000 ± 500 K blackbody-like emitter (e.g. Hawley & Fisher 1992). From this we estimate $\Delta V \sim -10$ and $\Delta U \sim -15$. This is consequently the second largest observed white-light flare from an L dwarf, following ASASSN-16ae ($\Delta V = -11$; Schmidt et al. 2016), and larger than those observed with *Kepler* (Gizis et al. 2013, 2017a; Paudel et al. 2018).

3.2 Flare energy

To calculate the flare energy we have again assumed the flare is given by a 9000 ± 500 K blackbody. We initially renormalise the blackbody to match the SDSS i'-band magnitude for each point in the calibrated flare amplitude light curve from Section 3.1. For each time step we integrate the corresponding renormalised flare blackbody over all wavelengths and multiply by $4\pi d^2$, where $d = 76^{+8}_{-7}$ pc, to calculate the bolometric flare luminosity. Finally, we integrate over the visible duration to calculate the total bolometric energy of the flare. This results in a bolometric flare energy of $3.4^{+0.9}_{-0.7} \times 10^{33}$ erg, which is over an order of magnitude greater than the energy of the Carrington event on the Sun (10^{32} erg; Carrington 1859; Tsurutani et al. 2003). Another way of analysing this is to compare it to the total bolometric luminosity of the star in quiescence. Integrating over our best-fitting SED results in a luminosity of 5.3×10^{29} erg s^{-1}, meaning the flare is equivalent in energy to 1.8 h of quiescent emission from ULAS J2249−0112. We note that this energy is only for the visible duration of the flare and is thus a lower limit.

4 DISCUSSION

We have detected a large amplitude white-light superflare on the L2.5 star ULAS J2249−0112. This is only the second L-dwarf flare to be detected from the ground and the sixth L-dwarf to have exhibited flaring activity. It is the coolest star ever found to exhibit a white-light flare. The flare had an amplitude of $\Delta V \sim -10$ and energy of $3.4^{+0.9}_{-0.7} \times 10^{33}$ erg, making it the second largest amplitude L dwarf flare, following that of ASASSN-16ae (Schmidt et al. 2016). With a cadence of 12 s this is the best resolved detection of a giant white-light flare, allowing direct measurements of the amplitude and duration without relying on extrapolation.

4.1 Magnetic activity of L dwarfs

The detection of a white-light flare from an L2.5 dwarf makes this the coolest star to show such an event and shows strong chromospheric activity can persist to this spectral type. Studies of the Hα emission from ultracool dwarfs using BOSS spectra (Schmidt et al. 2015) have found the activity strength $\log(L_{\rm H\alpha}/L_{\rm bol})$

to decrease from approximately −3.8 at the M4 spectral type towards −5.7 at L3. This decrease in Hα activity may imply the chromospheres of early L dwarfs are significantly cooler than their late M dwarf counterparts, or cover a smaller fraction of the surface (lower filling factor; Schmidt et al. 2015). Recent discoveries of mid-L dwarfs with Hα emission have shown this decrease in chromospheric strength seems to continue with spectral type (e.g. Pérez-Garrido, Lodieu & Rebolo 2017) and can be linked to the decreasing ionisation in the L dwarf photosphere (e.g. Miles-Páez et al. 2017). Ultracool dwarfs are also known to exhibit auroral activity (e.g. Kao et al. 2018), which may account for observed Hα emission in these systems. It is expected that the transition from predominantly chromospheric to auroral Hα emission occurs during the L spectral type (Pineda, Hallinan & Kao 2017). Many ultracool dwarfs that show activity such as radio emission and flaring also tend to be fast rotators, with rotation periods on the order of hours. However, neither the L1 dwarf SDSSp J005406.55−003101.8 (Gizis et al. 2017a) nor the L0 dwarf J12321827−0951502 (Paudel et al. 2018) showed any sign of rapid rotation when observed by *K2*, despite showing large amplitude white-light flares. Consequently, we do not attempt to predict whether ULAS J2249−0112 is a fast rotator. Regardless of this, studies of white-light flares such as from ULAS J2249−0112 can aid in understanding exactly how far into the L spectral type chromospheric activity persists.

4.2 Flare structure

In Section 3.1, we fitted the flare using a single continuous model, shown in Fig. 1. This model incorporates a Gaussian heating pulse with two exponential decays, for thermal and non-thermal cooling, respectively (Jackman et al. 2018). From our fit we can also identify the presence of a possible second peak. This is from an outlier lying 2.8σ from the fitted model and occurring approximately 40 s after the fitted peak. Multiple peaks in flares have previously been attributed to flares occurring on different parts of the star, and previous studies have found that higher energy flares are more likely to be complex (e.g. Hawley et al. 2014). One possibility for multiple peaks is sympathetic flaring, where one flare triggers flaring in different active regions (e.g. Moon et al. 2002). By assuming the flare is given by a 9000 K blackbody we can estimate the maximum area of emission. We estimate our flare has a maximum emitting area of 5.6×10^{19} cm^2, or 37 per cent of the visible hemisphere (e.g. Hawley et al. 2003). This value for the emitting area is similar to those for flares on M dwarfs (e.g. Osten et al. 2010), however, covers a much greater fraction of the surface. For example, a flare of similar energy observed by Hawley et al. (2003) from the M3.5 dwarf AD Leo (which had multiple peaks) had a covering fraction of ≈1 per cent. If we assume this emission area is related to the area of the flare footpoints (as in Osten et al. 2010) and that only flares of similar energy would cause visible substructure, then multiple flares with large footpoints on the stellar surface in quick succession would be required. This requirement may inhibit the presence of multiple peaks in L dwarf flares, suggesting the observed outlier is perhaps not due to a separate event. If this is the case, then the lack of complexity would make it similar to the $\Delta K_p = -5.4$ flare detected by Paudel et al. (2018) on the L0 dwarf 2MASS J12321827−0951502. This flare showed no obvious substructure other than an extended decay when observed in the *K2* 1 min short-cadence mode.

In Section 3.1, we measured the visible duration of ULAS J2249−0112 as 9.5 min. Along with this, we were able to measure the e-folding duration as 2.1 min, the $t_{1/2}$ duration as 1.5 min, and the FWHM of the Gaussian heating pulse as 12 s. Comparing the $t_{1/2}$ duration to other L dwarf flares, we find it is smaller than the three other large amplitude L dwarf flares (Schmidt et al. 2016; Gizis et al. 2017a; Paudel et al. 2018) and is more comparable to the smaller flares observed from the L1 dwarf WISEP J190648.47+401106.8 (e.g. Gizis et al. 2013). While this implies that this is the most rapid large amplitude flare observed from an L dwarf, we note that all large amplitude L dwarf flares have had $t_{1/2}$ values below 10 min. As such, other observations may have been hindered by the resolution of observations (as noted by Paudel et al. 2018) that would smear out flares in time (e.g. Yang et al. 2018). To estimate this effect we bin our data to cadences of 1 and 2 min, to simulate the *Kepler* and *Transiting Exoplanet Survey Satellite* (*TESS*) short-cadence modes. We measure $t_{1/2}$ time-scales of 2 and 3.25 min, respectively, showing that $t_{1/2}$ measurements can be significantly affected by the longer cadence of these space telescopes. The short duration of our flare thus highlights the requirement of high-cadence observations in order to detect and characterise these events. This behaviour would not be visible in the *TESS* 30 min cadence full-frame images (Ricker et al. 2015), nor in all-sky surveys that monitor large areas of sky each night. This shows how NGTS is in an ideal position to probe flare behaviour on the latest spectral types.

5 CONCLUSIONS

In this Letter, we have presented the detection of a giant white-light flare from the L2.5 star ULAS J224940.13−011236.9. The flare was detected from a dedicated search for stellar flares on low-mass stars in the NGTS full-frame images and has an amplitude of $\Delta i' \approx -6$, or $\Delta V \sim -10$. This makes it the second largest flare to be detected from an L dwarf and is the second to be detected from the ground. With a spectral type of L2.5 we believe ULAS J2249−0112 is the coolest star to show a white-light flare to date. This flare detection also highlights the value of the NGTS high-cadence full-frame images in studying the largest stellar flares from the coolest stars.

ACKNOWLEDGEMENTS

We are grateful to the referee, John Gizis, for helpful suggestions. This research is based on data collected under the NGTS project at the ESO La Silla Paranal Observatory. The NGTS facility is funded by a consortium of institutes consisting of the University of Warwick, the University of Leicester, Queen's University Belfast, the University of Geneva, the Deutsches Zentrum für Luft- und Raumfahrt e.V. (DLR; under the 'Großinvestition GI-NGTS'), the University of Cambridge, together with the UK Science and Technology Facilities Council (STFC; project reference ST/M001962/1). JAGJ is supported by STFC PhD studentship 1763096. PJW is supported by STFC consolidated grant ST/P000495/1. PE acknowledges the support of the DFG priority program SPP 1992 'Exploring the Diversity of Extrasolar Planets' (RA714/13-1). This publication makes use of data products from the Two Micron All Sky Survey, which is a joint project of the University of Massachusetts and the Infrared Processing and Analysis Center/California Institute of Technology, funded by the National Aeronautics and Space Administration and the National Science Foundation. This publication also makes use of data products from the *Wide-field Infrared Survey Explorer*, which is a joint project of the University of California, Los Angeles, and the Jet Propulsion Laboratory/California Institute of Technology, funded by the National Aeronautics and Space Administration.

REFERENCES

Allard F., Homeier D., Freytag B., 2012, Philos. Trans. R. Soc. Lond. Ser. A, 370, 2765
Benz A. O., Güdel M., 2010, ARA&A, 48, 241
Borucki W. J. et al., 2010, Science, 327, 977
Bramich D. M. et al., 2008, MNRAS, 386, 887
Burgasser A. J. et al., 2015, ApJS, 220, 18
Carrington R. C., 1859, MNRAS, 20, 13
Cutri R. M. et al., 2014, VizieR Online Data Catalog, II/328
Davenport J. R. A. et al., 2014, ApJ, 797, 122
Dawson K. S. et al., 2013, AJ, 145, 10
Dupuy T. J., Liu M. C., 2012, ApJS, 201, 19
Gaia Collaboration et al., 2018, A&A, 616, A1
Gillen E., Hillenbrand L. A., David T. J., Aigrain S., Rebull L., Stauffer J., Cody A. M., Queloz D., 2017, ApJ, 849, 11
Gizis J. E., Burgasser A. J., Berger E., Williams P. K. G., Vrba F. J., Cruz K. L., Metchev S., 2013, ApJ, 779, 172
Gizis J. E. et al., 2015, ApJ, 813, 104
Gizis J. E., Paudel R. R., Schmidt S. J., Williams P. K. G., Burgasser A. J., 2017a, ApJ, 838, 22
Gizis J. E., Paudel R. R., Mullan D., Schmidt S. J., Burgasser A. J., Williams P. K. G., 2017b, ApJ, 845, 33
Hawley S. L., Fisher G. H., 1992, ApJS, 78, 565
Hawley S. L. et al., 2003, ApJ, 597, 535
Hawley S. L., Davenport J. R. A., Kowalski A. F., Wisniewski J. P., Hebb L., Deitrick R., Hilton E. J., 2014, ApJ, 797, 121
Howell S. B. et al., 2014, PASP, 126, 398
Jackman J. A. G. et al., 2018, MNRAS, 477, 4655
Kao M. M., Hallinan G., Pineda J. S., Stevenson D., Burgasser A., 2018, ApJS, 237, 25
Lawrence A. et al., 2007, MNRAS, 379, 1599
Liebert J., Kirkpatrick J. D., Cruz K. L., Reid I. N., Burgasser A., Tinney C. G., Gizis J. E., 2003, AJ, 125, 343
Miles-Páez P. A., Metchev S. A., Heinze A., Apai D., 2017, ApJ, 840, 83
Moon Y.-J., Choe G. S., Park Y. D., Wang H., Gallagher P. T., Chae J., Yun H. S., Goode P. R., 2002, ApJ, 574, 434
Muirhead P. S., Dressing C. D., Mann A. W., Rojas-Ayala B., Lépine S., Paegert M., De Lee N., Oelkers R., 2018, AJ, 155, 180
Osten R. A. et al., 2010, ApJ, 721, 785
Paudel R. R., Gizis J. E., Mullan D. J., Schmidt S. J., Burgasser A. J., Williams P. K. G., Berger E., 2018, ApJ, 858, 55
Pérez-Garrido A., Lodieu N., Rebolo R., 2017, A&A, 599, A78
Pineda J. S., Hallinan G., Kao M. M., 2017, ApJ, 846, 75
Ricker G. R. et al., 2015, J. Astron. Telesc. Instrum. Syst., 1, 014003
Schmidt S. J., West A. A., Hawley S. L., Pineda J. S., 2010, AJ, 139, 1808
Schmidt S. J., Hawley S. L., West A. A., Bochanski J. J., Davenport J. R. A., Ge J., Schneider D. P., 2015, AJ, 149, 158
Schmidt S. J. et al., 2016, ApJ, 828, L22
Schmidt S. J. et al., 2018, preprint (arXiv:1809.04510)
Shibayama T. et al., 2013, ApJS, 209, 5
Skrutskie M. F. et al., 2006, AJ, 131, 1163
Skrzypek N., Warren S. J., Faherty J. K., 2016, A&A, 589, A49 (ULAS J2249−0112)
Stephens D. C. et al., 2009, ApJ, 702, 154
Tsurutani B. T., Gonzalez W. D., Lakhina G. S., Alex S., 2003, J. Geophys. Res. Space Phys., 108, 1268
Wheatley P. J. et al., 2018, MNRAS, 475, 4476
Wright E. L. et al., 2010, AJ, 140, 1868
Yang H., Liu J., Qiao E., Zhang H., Gao Q., Cui K., Han H., 2018, ApJ, 859, 87
York D. G. et al., 2000, AJ, 120, 1579

This paper has been typeset from a TEX/LATEX file prepared by the author.